Heterogeneous/Homogeneous Catalysis

DOI: 10.1002/ange.201301327

# Sustained Water Oxidation by a Catalyst Cage-Isolated in a Metal–Organic Framework**

*Binod Nepal and Siddhartha Das**

A significant challenge in sustainable energy research is to be able to devise systems to catalyze reactions at much higher scales than what is currently practiced for any other chemical process. Water oxidation and $CO_2$ reduction are the two reactions that carry pivotal importance for efficient solar-to-chemical energy conversion. However, the large-scale applicability, sustenance, and efficiency of these processes will be impossible without catalysts that not only have high turnover rates but also are long lasting, modular (for easy tailoring), and can be regenerated on demand.

In homogeneous, molecular catalysis, catalysts have modularity, but highly reactive catalysts are not long-lasting; they tend to undergo fast degradation. Even though ligand modification prevents degradation, it usually yields catalysts with lower turnover rates.[1] One iconic example, where degradation of a molecular catalyst could be prevented without affecting the catalytic efficiency, was the development of bulky heme-based catalysts by Collman and coworkers.[2] Incorporation of a bulky substituent on the phenyl groups of the tetraphenylporphyrin ligand could prevent inactivation of the heme-based catalysts by bimolecular interaction to form the Fe–O–O–Fe unit. This apparently simple modification has spurred a major development in heme-based oxidation catalysts. Recently, Kubiak and coworkers have reported a significant improvement in the activity of [Re(bipy)$(CO)_3$Cl]-based catalysts in $CO_2$ reduction by introducing a bulky substituent (*t*Bu), where prevention of the destructive intermolecular interactions was suggested to be one of the factors for this enhancement.[3]

Herein we report a simple yet efficient approach that prevents degradative side-reactions while sustaining catalyst turnover, resulting in highly sustained catalysis with minimized degradation. We utilize well-defined cages of a crystalline extended framework, the metal–organic framework (MOF) known as MIL-101(Cr),[4] to encage the molecules of a highly reactive water-oxidation catalyst containing a high-valent Mn(μ-O)$_2$Mn core (Figure 1). This cage isolation enables the catalyst to achieve water oxidation at a sustained high initial rate. The catalysis persists with the same turnover rate even after achieving a more than 20-fold higher total turnover number in water oxidation compared to its homogeneous state. In MIL-101(Cr), the apertures of the cages are too small for any migration of the catalyst to a neighboring cage; the cage itself is however large enough to provide the catalyst with the required catalytic environment. Thus, a catalyst molecule can remain isolated in the cage, where it functions like a homogeneous system but is separated from the bulk population of catalysts.

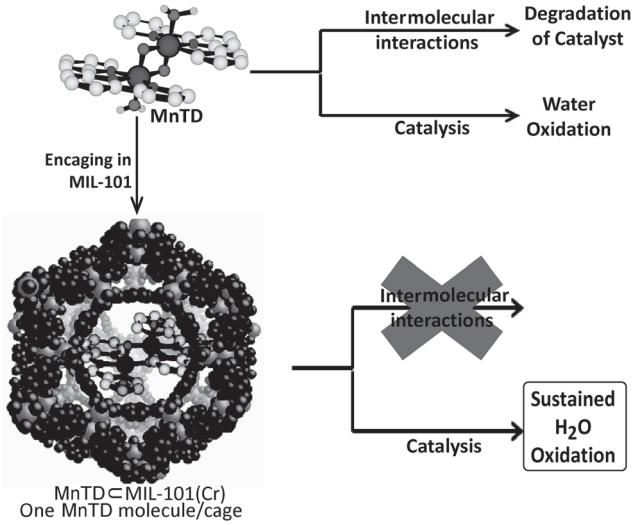


***Figure 1.*** Comparison of catalysis with MnTD molecules alone and encaging within the MOF, MIL-101(Cr), resulting in the MnTD⊂MIL-101(Cr) construct, leading to sustained water oxidation catalysis.

High-valent di-μ-oxo dimanganese catalysts have been studied thoroughly as functional mimics of the oxygen-evolving complex (OEC) in photosystem II (PS II).[1,5] MnTD ([(terpy)Mn(μ-O)$_2$Mn](terpy)]$^{3+}$; terpy: 2,2′:6′,2″-terpyridine) is not only among the best homogeneous water-oxidation catalysts (homogeneous) with an earth-abundant metal, but also structurally very similar to the OEC.[6]

Interestingly, while kinetic studies reveal that the major degradation pathways for MnTD require more than one MnTD molecule, the catalysis is first-order with respect to the catalyst.[6c] Rapid degradation causes only 5% of total catalyst to remain active as early as the onset of catalysis. Addition of substituents on the terpy (such as *t*Bu) has been found to either prevent the assembly of the Mn(μ-O)$_2$Mn core, or slow down the catalytic rate.[1] Previously, intermolecular interactions were decreased by immobilization of MnTD on a solid surface. This approach showed promise for water oxidation under photochemical,[7] photoelectrochemical,[8] and highly acidic conditions[9] (which causes degradation of the catalyst in the homogeneous form;[10] however, immobilization on a solid surface cannot control, and therefore prevent, the

[*] B. Nepal, Dr. S. Das
Department of Chemistry and Biochemistry, Utah State University
Logan, UT 84322 (USA)
E-mail: Siddhartha.das@usu.edu

[**] We thank Utah State University for a start-up fund and Sanjit Das (graduate student) for helping with IR spectra.

Supporting information for this article is available on the WWW under http://dx.doi.org/10.1002/anie.201301327.

undesired intermolecular interactions between two MnTD molecules.

This motivated us to investigate the possibility of shutting down the detrimental intermolecular reactions of the catalyst without ligand modification. Below, we first discuss the structural aspect of the design, the synthetic strategy, and finally, the catalytic evaluation of our construct, respectively.

From the crystal structure of MnTD,[6b] we derived that a molecule of MnTD is box-shaped with dimensions of circa $14 \times 12 \times 8$ Å$^3$, plus the counterions.

MOFs present the prospect of a heterogeneous host, providing the liberty to plan and engineer well-defined pores with apertures of desired choice.[11] Among MOFs with first-row earth-abundant transition metals, those with $(\mu_3\text{-O})Cr_3(COO)_6$ as inorganic nodes were the most suitable to encage MnTD, as they were previously shown to be stable in highly oxidizing and acidic conditions.[12] Many of these MOFs have phenyl ring based struts (organic linkers) that are highly resilient to oxidation with MnTD.

The MIL-101(Cr) is a well-characterized MOF that comprises $(\mu_3\text{-O})Cr_3(COO)_6$ as the inorganic nodes and 1,4-benzene dicarboxylate (BDC) as the linker.[4] It has two types of mesoporous cages with maximum internal diameters of 29 Å and 34 Å, and pore apertures with maximum free diameters of 12 Å and 15 Å; in reality the available space is much smaller than these owing to the van der Waals radius of the π-cloud of the phenyl rings and solvent molecules. It is found that MIL-101(Cr), even when completely dried, carries 25 moles of $H_2O$ per mole of tri-Cr unit.[4] Therefore, we assumed that only one molecule of the MnTD can be assembled in one cage. The apertures, especially after subtracting 4 Å for aromatic π-cloud that borders it, make it impossible for the MnTD to diffuse out of the cage. MIL-101(Cr) was synthesized following literature procedure[4] and was activated following a slightly different activation method (see the Supporting Information).

As apertures of MIL-101(Cr) are smaller than MnTD, preassembled MnTD could not be infiltrated into the MOF. Thus, MnTD was assembled within the cages of MIL-101(Cr) as the catalytically active, high-valent manganese dimer. Assembly of MnTD requires precise control over kinetics and the stoichiometry of all the reagents; that is, terpy, $Mn^{II}$-salt, and K-oxone ($KHSO_5$). With MIL-101(Cr), the aperture was just the right size for starting materials to diffuse in without any significant mass-transfer problem. However, this problem of mass transfer prevented us from using other MOFs with similar tri-Cr unit with smaller cages and apertures (for example, MIL-100(Cr); linker: 1,3,5-benzene tricarboxylate).[13] MnTD⊂MIL-101(Cr) was synthesized by first loading the cages with terpy over a period of 18 h, followed by addition of $Mn(OAc)_2$ and, in parallel, K-oxone in stoichiometric amounts. The sample was washed with water repetitively to remove any unencaged MnTD. The similarity in the powder X-ray diffraction spectrum of synthesized MIL-101(Cr) and MnTD⊂MIL-101(Cr) indicated the maintenance of the structure of the extended framework (Figure 2a). The color of the sample underwent an obvious change from MIL-101(Cr) (light green) to MnTD⊂MIL-101(Cr) (dark green; similar to molecular MnTD). The FTIR spectrum of

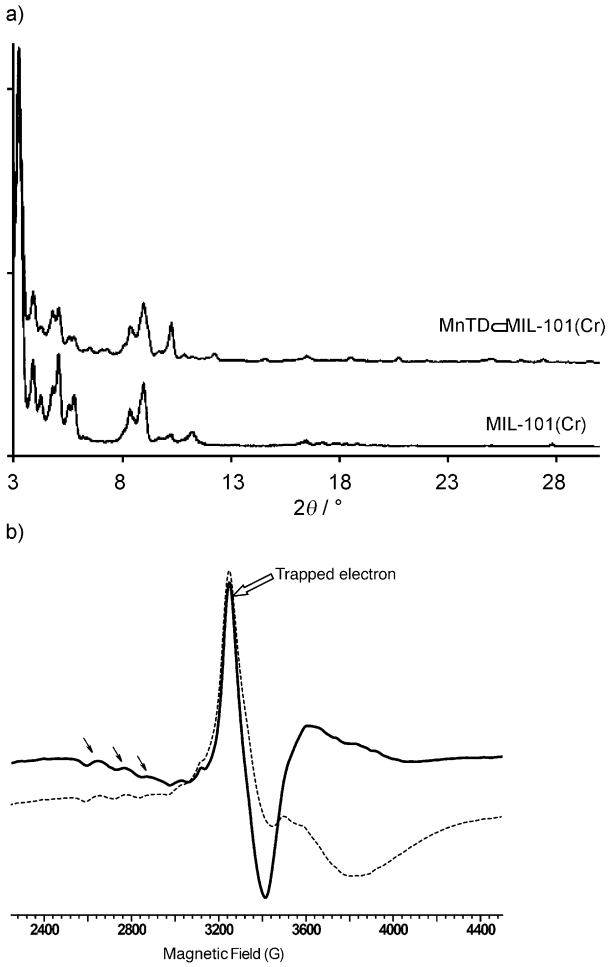


***Figure 2.*** a) PXRD pattern for MnTD⊂MIL-101(Cr) and MIL-101(Cr), indicating that the crystal structure is maintained in MnTD⊂MIL-101(Cr). b) EPR spectra of MnTD⊂MIL-101(Cr) (-----) and of MnTD⊂MIL-101(Cr)with peaks from MIL-101(Cr) subtracted (——) at 7 K (a strong signal from trapped electrons is present). The arrows mark the representative hyperfine lines arising from the coupled nuclear spin from $Mn^{III}$–$Mn^{IV}$ core.

MnTD⊂MIL-101(Cr) showed the characteristic about 775 cm$^{-1}$ arising from $Mn^{III}(\mu\text{-O})_2Mn^{IV}$ core. EPR (7 K) of MnTD⊂MIL-101(Cr) showed the 16-line spectrum characteristic of MnTD overlying the broad peak from tri-$Cr^{III}$ center (Figure 2b). The absence of EPR signals characteristic of $Mn^{II}$ species and of IR peaks characteristic of manganese oxides is indicative of the fact that high-valent MnTD is the most dominant manganese species in the system, which is also supported by our elemental analysis.

We reduced the high-valent MnTD to $Mn^{II}$ species by treating the MnTD⊂MIL-101(Cr) with dilute HCl; the resulting strong EPR signal (Supporting Information, Figure S6) from $Mn^{II}$ is distinctly different from the EPR spectrum in Figure 2b, ruling out any significant presence of $Mn^{II}$ species in MnTD⊂MIL-101(Cr) (although in the synthesis of $Mn^{III}/Mn^{IV}$ MnTD, $Mn^{II}$ is always found as a minor paramagnetic impurity[14]). $Mn_2^{IV/IV}$ is a catalytically inactive high-valent di-manganese species;[5] this species is of dark red color with a strong UV/Vis absorption between 400–520 nm

centering at about 460 nm (Supporting Information, Figure S7), whereas $Mn_2^{III/IV}$ is dark green with no absorbance in this region.[6b] Our synthesized MnTD⊂MIL-101(Cr) does not match the color of $Mn_2^{IV/IV}$ (Supporting Information, Figure S7), nor does it show the absorbance, expected from a $Mn_2^{IV/IV}$, in the UV/Vis spectrum (Supporting Information, Figure S8).

We quantified MnTD in MIL-101(Cr) by a) elemental analysis, b) comparing the mass losses in TGA experiments, and c) digesting a measured amount of MnTD⊂MIL-101(Cr) and UV/Vis quantification of the released species (see the Supporting Information). All analyses yielded about 10 wt% MnTD with respect to total MnTD⊂MIL-101(Cr). This is consistent with an average of about one molecule of MnTD per cage of MIL-101(Cr).[4] Further studies are under way to develop spectroscopic techniques for specific and unequivocal quantification of molecules of MnTD in pores (as opposed to average measurements).

Catalytic water oxidation measurements were carried out in a double-walled glass chamber equipped with circulating water bath to maintain the temperature at 25 °C. A 6 mL solution of MnTD and a suspension of MnTD⊂MIL-101(Cr) or a suspension of MIL-101(Cr) in acetate buffer was added to the chamber. A solution of K-oxone ($KHSO_5$) was also added as the terminal electron acceptor. Evolved $O_2$ was quantified by a Clark-type oxygen electrode fitted to the sample chamber with an airtight Delrin collar. The amount of molecular MnTD used for each catalysis is equivalent to the calculated amount of MnTD in MnTD⊂MIL-101(Cr) (equivalent to one-tenth of the total mass of MnTD⊂MIL-101(Cr)).

With molecular MnTD, high rates of $O_2$ evolution was recorded for about the first 200 s (Figure 3, inset; turnover frequency (TOF) = 0.04 mol $O_2$ (mol catalyst)$^{-1}$ s$^{-1}$) which slowed down and almost completely stopped after 400 s; however, MnTD⊂MIL-101(Cr) continued producing oxygen at the same initial rate till our Clark-type electrode was saturated with the produced $O_2$. At this point, the MnTD⊂MIL-101(Cr) was untouched, but the solution deoxygenated and a second aliquot of K-oxone (two-fifths of the initial amount) was added to the chamber. The $O_2$ evolution was observed to continue at the same high rate. This process was repeated ten times with the same sample of MnTD⊂MIL-101(Cr). There was no indication of a decrease in its catalytic rate. The rate of catalysis is somewhat lower, with a TOF of about 0.02 mol $O_2$ (mol caged MnTD·species)$^{-1}$, than the initial rate with molecular MnTD; this is expected from a real-time analysis of the catalytic rate, where mass-transfer is an issue. Molecular MnTD under identical conditions did not show any sustained $O_2$ evolution beyond the initial surge, even after addition of a fresh solution of K-oxone (same as described above). Control experiments with a) only K-oxone (without catalyst) and b) K-oxone + MIL-101(Cr) did not show any significant $O_2$ evolution.

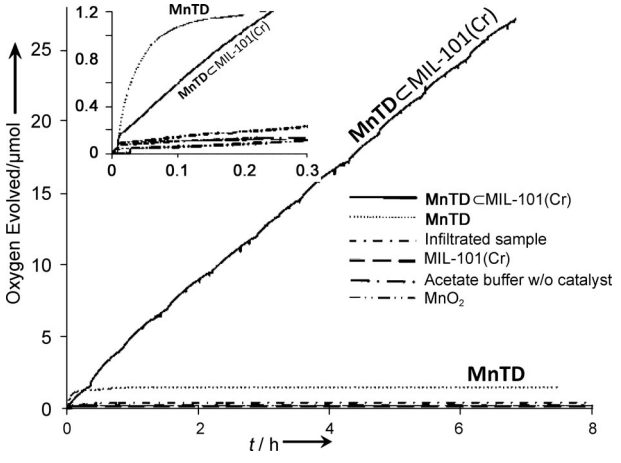


***Figure 3.*** Oxygen evolution plots for 2 mg of MnTD⊂MIL-101(Cr) (black), 0.19 μmole of MnTD, 2 mg of MIL-101, 5 mg $MnO_2$ and 2 mg of infiltrated sample in 6 mL acetate buffer (pH 4.5, 0.23 M) with 250 μL K-oxone (200 mM). In the case of MnTD⊂MIL-101(Cr), 100 μL K-oxone (200 mM) was added every time after the solution was deoxygenated with $N_2$.

The amount of MnTD loaded in MnTD⊂MIL-101(Cr) was quantified by elemental analysis, TGA, and UV/Vis spectroscopy (discussed above and in the Supporting Information) to be 10% (w/w) of the mass of MnTD⊂MIL-101(Cr). The equivalent weight of pure molecular MnTD was measured ($m = 0.2$ mg) and used in our control catalytic experiments (Figure 3). It should be noted that the analytical quantification techniques would not distinguish the catalytically active and inactive forms of Mn. Thus, the amount of MnTD used in the control experiment could be marginally higher than the active form of MnTD present in MnTD⊂MIL-101(Cr). Therefore, the actual catalytic enhancement owing to cage isolation could be higher than the amount reported herein.

Manganese oxides have been reported to show electrochemical water oxidation.[14] Under our catalytic conditions, $MnO_2$ did not show any $O_2$ production significantly above background levels (Figure 3, inset). The catalytic curve is monophasic, which is consistent with no drastic change in catalytic species throughout the measurement. This is quite different from what we see with the molecular MnTD. Moreover, the IR spectrum and PXRD of the sample after eight-hour catalysis did not show any peak that is characteristic of manganese oxides; instead, the IR spectrum contained the peak for the Mn(μ-O)$_2$Mn-core (see the Supporting Information).

Instead of the catalyst inside the pore performing the catalysis, either catalyst adsorbed on the surface of MIL-101(Cr) or slowly leached catalyst could be performing the catalysis. To address the first question, we soaked MIL-101(Cr) particles in a concentrated solution of preassembled MnTD in acetate buffer (note: for MnTD⊂MIL-101(Cr), MnTD was assembled from its starting materials inside the pore). Upon washing, the material did show some color change (light gray to very light green; Supporting Information, Figure S8) owing to the surface-adsorbed MnTD, but failed to show any sustained catalysis (Figure 3). To address the latter concern, we soaked a sample of MnTD⊂MIL-101(Cr) in acetate buffer overnight, and checked the supernatant solution for catalysis; this did not show any $O_2$ evolution. Supernatant solutions from the catalytic suspen-

  

sion of MnTD⊂MIL-101(Cr) also did not show any $O_2$ evolution, nor any UV/Vis absorption.

When catalysis is performed inside porous materials, there is always a question as to whether the catalysis is limited to the pores near the material surface. With the same MOF, MIL-101(Cr) with multiple encaged PTA units (PTA: phosphotungstic acid), Hatton and co-workers have reported unchanged catalytic rates upon variation of the MIL-101(Cr) particle size.[16] With MIL-101(Cr) with encaged PTA units, the study reports the catalytic rates for Baeyer condensation of benzaldehyde and 2-naphthol, the three-component condensation of benzaldehyde, 2-naphthol, and acetamide, and the epoxidation of caryophyllene by aqueous $H_2O_2$ composites: rates were independent of the MIL-101(Cr) particle size. As the reactants used in our case, K-oxone and water, are smaller in size, comparable in polarity, and more abundant than in this previous work, we do not anticipate any significant hindrance in the movement of reactants through the pores. However, MOF surfaces are known for their high affinity for gaseous molecules (such as $O_2$ adsorption by Cr-based MOFs[17]) and adsorption of some of the evolved $O_2$ by internal surfaces of MOFs, especially at the onset of catalysis, is possible.

It is often suggested that encapsulated catalysts tend to show enhanced activity owing to the higher local concentration of substrates, reagents, and catalyst.[18] As we do not notice any improvement in TOF, it is unlikely that the above phenomenon is playing a significant role in this specific system.

Electrochemical and photoelectrochemical water oxidation with MnTD have so far been largely hindered by fast bimolecular degradation of the catalyst; these studies will now be possible with our developed strategy, which is applicable to all catalyst systems.

In conclusion, we show the assembly of a highly reactive molecular catalyst (MnTD) that is prone to undergo destructive intermolecular interactions within well-defined pores of a MOF (metal: Cr). The pores, along with the apertures of the MOF, are designed to prevent diffusion of the catalyst molecules to a neighboring pore or diffuse out. This modular construct with earth-abundant materials could improve the turnover number of the water oxidation catalyst more than twentyfold while still sustaining the catalysis at its initial high rate. The net catalyst system is heterogeneous, but the catalyst itself performs homogeneous water oxidation in the isolating cages. We feel that the simplicity and the universality of this approach will be highly useful for taking the molecular catalysts a leap forward.

Received: February 14, 2013
Revised: April 11, 2013
Published online: May 31, 2013

**Keywords:** heterogeneous catalysis · mesoporous materials · metal–organic frameworks · reactive intermediates · water splitting

[1] H. Y. Chen, R. Tagore, S. Das, C. Incarvito, J. W. Faller, R. H. Crabtree, G. W. Brudvig, *Inorg. Chem.* **2005**, *44*, 7661 – 7670.
[2] J. P. Collman, R. R. Gagne, T. R. Halbert, J. C. Marchon, C. A. Reed, *J. Am. Chem. Soc.* **1973**, *95*, 7868 – 7870.
[3] E. E. Benson, C. P. Kubiak, *Chem. Commun.* **2012**, *48*, 7374 – 7376.
[4] G. Ferey, C. Mellot-Draznieks, C. Serre, F. Millange, J. Dutour, S. Surble, I. Margiolaki, *Science* **2005**, *309*, 2040 – 2042.
[5] a) S. Das, G. W. Brudvig, R. H. Crabtree, *Inorg. Chim. Acta* **2009**, *362*, 1229 – 1233; b) R. Tagore, R. H. Crabtree, G. W. Brudvig, *Inorg. Chem.* **2007**, *46*, 2193 – 2203; c) C. W. Cady, R. H. Crabtree, G. W. Brudvig, *Coord. Chem. Rev.* **2008**, *252*, 444 – 455.
[6] a) Y. Umena, K. Kawakami, J.-R. Shen, N. Kamiya, *Nature* **2011**, *473*, 55 – U65; b) J. Limburg, J. S. Vrettos, L. M. Liable-Sands, A. L. Rheingold, R. H. Crabtree, G. W. Brudvig, *Science* **1999**, *283*, 1524 – 1527; c) J. Limburg, J. S. Vrettos, H. Y. Chen, J. C. de Paula, R. H. Crabtree, G. W. Brudvig, *J. Am. Chem. Soc.* **2001**, *123*, 423 – 430; d) R. Tagore, R. H. Crabtree, G. W. Brudvig, *Inorg. Chem.* **2008**, *47*, 1815 – 1823.
[7] M. Yagi, M. Toda, S. Yamada, H. Yamazaki, *Chem. Commun.* **2010**, *46*, 8594 – 8596.
[8] R. Liu, Y. Lin, L.-Y. Chou, S. W. Sheehan, W. He, F. Zhang, H. J. M. Hou, D. Wang, *Angew. Chem.* **2011**, *123*, 519 – 522; *Angew. Chem. Int. Ed.* **2011**, *50*, 499 – 502.
[9] a) M. Yagi, K. Narita, *J. Am. Chem. Soc.* **2004**, *126*, 8084 – 8085; b) G. Li, E. M. Sproviero, R. C. Snoeberger III, N. Iguchi, J. D. Blakemore, R. H. Crabtree, G. W. Brudvig, V. S. Batista, *Energy Environ. Sci.* **2009**, *2*, 230 – 238; c) P. Kurz, *Dalton Trans.* **2009**, 6103 – 6108; d) H. Yamazaki, S. Igarashi, T. Nagata, M. Yagi, *Inorg. Chem.* **2012**, *51*, 1530 – 1539.
[10] R. Tagore, H. Y. Chen, H. Zhang, R. H. Crabtree, G. W. Brudvig, *Inorg. Chim. Acta* **2007**, *360*, 2983 – 2989.
[11] a) Z. Wang, S. M. Cohen, *Chem. Soc. Rev.* **2009**, *38*, 1315 – 1329; b) J. Lee, O. K. Farha, J. Roberts, K. A. Scheidt, S. T. Nguyen, J. T. Hupp, *Chem. Soc. Rev.* **2009**, *38*, 1450 – 1459; c) S. M. Cohen, *Chem. Rev.* **2012**, *112*, 970 – 1000; d) O. K. Farha, J. T. Hupp, *Acc. Chem. Res.* **2010**, *43*, 1166 – 1175; e) D. J. Tranchemontagne, J. L. Mendoza-Cortes, M. O'Keeffe, O. M. Yaghi, *Chem. Soc. Rev.* **2009**, *38*, 1257 – 1283.
[12] S. Das, D. E. Johnston, S. Das, *CrystEngComm* **2012**, *14*, 6136 – 6139.
[13] G. Férey, C. Serre, C. Mellot-Draznieks, F. Millange, S. Surble, J. Dutour, I. Margiolaki, *Angew. Chem.* **2004**, *116*, 6456 – 6461; *Angew. Chem. Int. Ed.* **2004**, *43*, 6296 – 6301.
[14] S. R. Cooper, M. Calvin, *J. Am. Chem. Soc.* **1977**, *99*, 6623.
[15] F. Jiao, H. Frei, *Energy Environ. Sci.* **2010**, *3*, 1018 – 1027, and references therein.
[16] L. Bromberg, Y. Diao, H. Wu, S. A. Speakman, T. A. Hatton, *Chem. Mater.* **2012**, *24*, 1664 – 1675.
[17] L. J. Murray, M. Dinca, J. Yano, S. Chavan, S. Bordiga, C. M. Brown, J. R. Long, *J. Am. Chem. Soc.* **2010**, *132*, 7856 – 7857.
[18] B. Li, S. Bai, X. Wang, M. Zhong, Q. Yang, C. Li, *Angew. Chem.* **2012**, *124*, 11685 – 11689; *Angew. Chem. Int. Ed.* **2012**, *51*, 11517 – 11521.

  